Rev. Roum. Sci. Techn.– Électrotechn. et Énerg.
Vol. **69**, *3*, pp. 305–310, Bucarest, 2024

DESIGN AND REAL-TIME IMPLEMENTATION OF SYNERGETIC REGULATOR FOR A DC-DC BOOST CONVERTER

SAMIA LATRECHE[1], BADREDDINE BABES[2,*], AMAR BOUAFASSA[3]

Keywords: DC-DC boost converter; Synergetic voltage regulator; Lyapunov approach; Grid disturbances.

Switching DC/DC boost converters are one of the most economical devices for increasing supply voltage due to their large conversion efficiency. With the development of modern control technologies, control of DC/DC converters has become increasingly important to improve system power density and efficiency. The output voltage of these power converters must meet stringent specifications to be fast and stable. To regulate the DC/DC boost converter in the presence of disturbances, a synergistic control (SC) system derived from synergistic theory is presented in this study. Based on the state variables, the total variable manifold supports the proposed control scheme. The distinctive features of the SC system via sliding mode control are finite time convergence and chattering-free phenomena. The Lyapunov approach is used to examine the stability of the controlled system. The suggested control scheme was verified by simulation and experimentally validated using a dSPACE DS1104 card. The controller exhibits a suitable response with high performances, such as fast transient response, negligible steady-state error, and better performance under load and output voltage fluctuations.

1. INTRODUCTION

The widespread use of EVs [1, 2], batteries [3], renewable energies like PV [4, 5], and microgrids [6] has encouraged the rapid development of power converters to meet dynamic load demands and strict requirements on the power supply. Among all the developed power converters, step-up DC/DC converters are attractive for different applications supplied by DC output voltage power sources. These converters have the advantages of high efficiency, smooth waveforms, and an extremely high power density. Non-linearity and time-varying systems are important phenomena that deteriorate the performance of DC/DC converters. The DC/DC boost converter control is usually challenging to regulate the output voltage and ensure robustness over a wide range of parametric and load changes.

Linear PI-based control strategies are still the prevailing control strategies that rely heavily on the rated parameters of the controlled systems. Due to their shortcomings, several enhanced control schemes for DC/DC converters have been developed, such as sliding mode control (SMC) [7–10], predictive control [11,12], LMI-based robust controller [13], fuzzy logic controller [14], synergetic control (SC) [15], and so on.

When facing unexpected disturbances, robust control design is considered a topic of significant research interest. Ensuring the system's stability and robustness during parameter changes is still challenging. Recently, the SC has emerged as a promising control owing to its ease of implementation for controlling the DC/DC converters [15]. The Russian researcher Kolesnikov developed the SC scheme [16] and has aroused several applications in power electronics and various industrial processes [17–21]. It is based on the ideas of modern mathematics and synergetics. The SC shares some features with SMC to force the closed-loop system to move on a desired manifold. Compared to SMC, the chattering phenomenon is handled better in SC, which can track the system references in a finite time. However, the SC requires the complete mathematical model of the controlled system.

Considering the literature review, it is obvious that researchers constantly develop different cost-effective controllers without sacrificing performance. For this reason, this paper outlays the analysis and real-time implementation based on the dSPACE 1104 card of an efficient boost converter with a cost-effective scheme based on SC theory. As it is well known, the DC/DC boost converter lacks advancements in two different standpoints. The first hurdle is the switching losses. The second one is the inability to maintain the desired performance due to internal parameter changes and external disturbances. The proposed control scheme investigated in this paper attempts to mitigate the issues above, which will make the fast-tracking of output voltage and enhance the conversion ratio.

Therefore, this paper is arranged as follows: The second section describes the DC/DC boost converter model as a built-in simulation. The third section explains the basic principle of the SC. The results of the simulation and the experiments are reported in sections 4 and 5, respectively. Final remarks can be found in section 6.

2. MODELING OF THE CONVERTER CIRCUIT

Figure 1 shows the conventional electronic circuit of a DC/DC boost converter. It mainly consists of a DC input voltage (V_{in}), a controlled switch (S), a diode (D) acting as a free-wheeling diode, an inductor (L), a capacitor (C), and a load resistor (R).

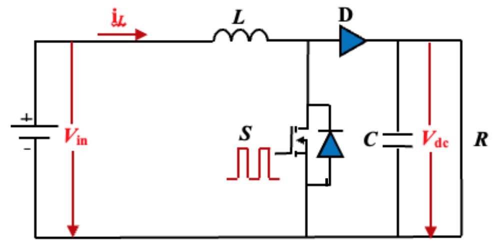

Fig. 1 – Typical structure of the step-up boost converter.

The dynamic model of the boost type converter is given by [8]:

$$\begin{cases} \dfrac{\mathrm{d}i_L}{\mathrm{d}t} = -\dfrac{V_{dc}}{L}(1-d) + \dfrac{1}{L}V_{in} \\ \dfrac{\mathrm{d}V_{dc}}{\mathrm{d}t} = \dfrac{i_L}{C}(1-d) - \dfrac{V_{dc}}{RC} \end{cases} \quad 0 \le d \le 1, \quad (1)$$

where V_{in} and V_{dc} are the input and output voltage, respectively, and d is the control signal.

[1] Technology Faculty, Electrical Engineering Department, Automation Laboratory of Setif, University of Setif 1, Algeria
[2,*] Research Center in Industrial Technologies CRTI, Algiers, Algeria
[3] LGEPC Laboratory, National Polytechnic School of Constantine, Constantine, Algeria
E-mails: samia.latreche@univ-setif.dz, b.babes@crti.dz (correspondence), amar.bouafassa@enp-constantine.dz

DOI: 10.59277/RRST-EE.2024.69.3.9

3. BRIEF SURVEY OF SC THEORY

The SC technique provides valuable ideas for controlling systems with various uncertainties, time-varying parameters, disturbances, *etc*. Moreover, it is used to avoid chaotic behavior and enhance the quality of regulation in power electronics applications [16, 17]. It is close to SMC because it forces the system to evolve on a pre-selected manifold. The main advantage of SC over the SMC is that it eliminates chattering phenomena. The control uses a macro-variable that can be a function of the system's two or more state variables. By the appropriate choice of macro-variables, the designer can obtain a powerful method to improve tracking accuracy for the final system by (i) ensuring the overall stability of the system, (ii) insensitive to fluctuations or parameter variations, and (*iii*) noise suppression. Consider the nonlinear SISO system that is expressed as follows:

$$\frac{\mathrm{d}x(t)}{\mathrm{d}t} = f(x,u,t), \tag{2}$$

where $x \in \mathrm{R}^n$ represents the state variable and $u \in \mathrm{R}^m$ represents the control variables. The SC synthesis consists of the following three steps:

- Step1: Choice of a function based on the state variable of the system named macro variable:

$$\psi = \psi(x,t), \tag{3}$$

The main objective of the macro variable is to force the system to evolve on a pre-selected manifold $\psi = 0$. The operator can select the characteristics of the macro variable, considering some parameters such as the control objective, response time, and control limitations [22–26].

- Step 2: Definition of the dynamic evolutions of the macro-variables to ensure the desired constraints, which can be expressed by eq. (4):

$$T\dot{\psi} + \psi = 0, \quad T > 0, \tag{4}$$

where T is a positive control parameter that indicates the closed-loop system's convergence rate to the desired equilibrium point, the solution of eq. (3) is given as:

$$\psi(t) = \psi_0 \mathrm{e}^{\frac{-t}{T}}, \tag{5}$$

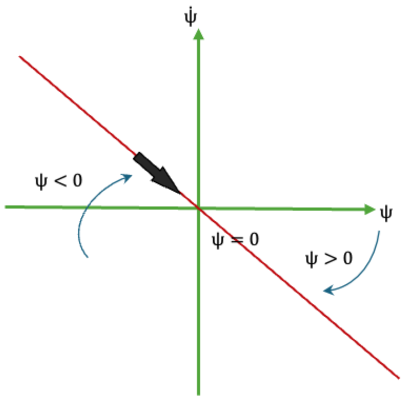

Fig. 2 – SC in phase portrait.

It is obvious that $\psi(t)\to 0$ at $t\to\infty$.

The system operating point converges to the straight line (control manifold) and then moves to the origin point, as shown in Fig. 2.

- Step 3: Synthesis of the control law.

Considering the differentiation chain, it gives:

$$\dot{\psi} = \frac{\mathrm{d}\psi(x,t)}{\mathrm{d}t} = \frac{\mathrm{d}\psi(x,t)}{\mathrm{d}x}\cdot\frac{\mathrm{d}x(t)}{\mathrm{d}t}, \tag{6}$$

Substituting eq. (2) and (3) into eq. (4), it is derived:

$$T\frac{\mathrm{d}\psi(x,t)}{\mathrm{d}x} f(x,u,t) + \psi(x,t) = 0, \tag{7}$$

From eq. (6) the control law can be expressed as:

$$u = g(x,\psi(x,t),T,t), \tag{8}$$

3. CONTROL DESIGN OF SC ALGORITHM

Control techniques play a vital role in optimizing the overall operations of the boost converter to attain high system performance. A nonlinear control law based on the SC technique is synthesized in this section to regulate the output DC-link voltage of the step-up boost converter.

The output voltage and its derivative are chosen as the state variable of the system:

$$\begin{cases} x_1 = i_l \\ x_2 = V_{\mathrm{dc}} \end{cases}. \tag{9}$$

If d is assumed as the duty ratio of a switching period, the average model of the boost converter can be expressed by:

$$\begin{cases} \dot{x}_1 = -\frac{x_2}{L}(1-d) + \frac{1}{L}V_{\mathrm{in}} \\ \dot{x}_2 = \frac{x_1}{C}(1-d) - \frac{x_2}{RC} \end{cases} \quad 0 \le d \le 1, \tag{10}$$

The output voltage and current errors are defined as follows:

$$\begin{cases} e_1 = x_1 - i_{l\mathrm{ref}} \\ e_2 = x_2 - V_{\mathrm{dc\_ref}} \end{cases}, \tag{11}$$

where $V_{\mathrm{dc\text{-}ref}}$, $i_{\mathrm{l\_ref}}$ are the reference output voltage and reference current respectively under the constraint such that $\lim_{t\to\infty}\|x_{\mathrm{i}} - x_{\mathrm{i\_ref}}\| \to 0,\ i = 1{,}2$. A macro-variable ψ of the SC can be expressed as:

$$\psi = e_1 + \mathrm{K}e_2 = V_{\mathrm{dc}} - V_{\mathrm{dc\_ref}} + K(i_{\mathrm{l}} - i_{\mathrm{l\_ref}}), \tag{12}$$

where K is a positive constant chosen by the designer, the macro-variables constraint is chosen by:

$$T\dot{\psi} + \psi = 0; \quad T > 0, \tag{13}$$

Differentiating eq. (12), then it is obtained:

$$\dot{\psi} = \dot{x}_2 + K\dot{\mathrm{x}}_1, \tag{14}$$

From eqs. (10), (13) and (14), then it can be derived:

$$T\left[\frac{x_1}{C}(1-d) - \frac{x_2}{RC} + K\left(-\frac{x_2}{L}(1-d) + \frac{1}{\mathrm{L}}V_{\mathrm{in}}\right)\right] + \psi = 0 \tag{15}$$

Then, the SC law defines the control signal (d) as:

$$d = 1 - \left[\frac{\frac{K}{L}V_{\text{in}} - \frac{x_2}{RC} + \frac{x_2 - x_{2\_\text{ref}}}{\text{T}} + \frac{K(x_1 - x_{1\_\text{ref}})}{\text{T}}}{\frac{K}{L}x_2 - \frac{1}{C}x_1}\right], \quad (16)$$

The Lyapunov analysis is used to prove the stability.

Assuming:

$$V = \frac{1}{2}\psi^{\mathrm{T}}\psi, \quad (17)$$

Therefore:

$$\dot{V} = \psi^{\mathrm{T}}\psi, \quad (18)$$

From eq. (11), it leads to:

$$V = -\frac{1}{T}\psi^2;\ T > 0, \quad (19)$$

Thus $V \leq 0$.

According to the Lyapunov theory, the system stability under the control law is guaranteed, and the trajectory converges at an infinite time to the equilibrium point.

4. SIMULATION RESULTS

This section is intended to compare the performances of the suggested SC algorithm and PID controller. Numerical simulations under different load and output voltage variations have been performed using MATLAB/Simulink software. The specifications of the DC-DC boost converter utilized in this work are summarized in Table 1.

The switching frequency (f_s) is fixed at 20 kHz. When V_{in} is 20 V, the duty cycle D is 0.6, and the inductor current variation Δi_L is 0.03 A. Therefore, the inductor L is determined by

$$L = \frac{V_{\text{in}}D}{f_s \Delta i_L} = 20\ \text{mH}. \quad (20)$$

Table 1

Parameters of the circuit

Parameters	Values
Input voltage (V_{in})	20 V
Reference output voltage ($V_{dc\text{-}ref}$)	40 V
DC-bus capacitor (C)	1100 µF
Input inductance (L)	20 mH
Load resistance (R)	100 Ω
Sampling time (T_s)	50.10^{-6} s
Switching frequency (f_s)	20 kHz

In this article, three types of system testing are utilized. The first system test is a step reference voltage change. This test evaluated the suggested SC algorithm and PID controller capabilities to track and maintain the reference output voltage level.

Figure 3 presents the simulation results of the suggested SC algorithm and PID controller for a DC-DC boost converter with a fixed output voltage of 40 V and a fixed resistive load of 100 Ω.

As shown in Fig. 3, the suggested SC algorithm performs excellently in tracking the reference output voltage ($V_{dc\text{-}ref}$) when the setpoint changes. The algorithm demonstrates commendable performance in maintaining the desired value perfectly.

The suggested SC algorithm does not overshoot in the starting condition, but the PID controller overshoots around 49.89 V.

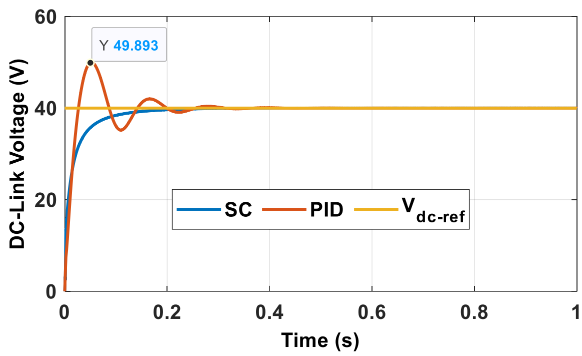

Fig. 3 – Step responses of the suggested SC algorithm and PID controller for DC-DC boost converter with fixed load.

The second system test is a step reference voltage change. During the time [1, 2] s, a step change in the reference output voltage from 40 V to 80 V and inversely from 80 V to 40 V takes place to evaluate the robustness of the suggested SC scheme and PID controller. Figure 4 shows the tracking ability of the proposed SC algorithm and PID controller.

Figure 4 shows that the SC algorithm performs better than the PID controller regarding overshoot, undershoot, and transient response. In addition, the output DC-link voltage is unaffected and tracks its reference values perfectly with a fast response time, which illustrates the robustness of the suggested SC algorithm.

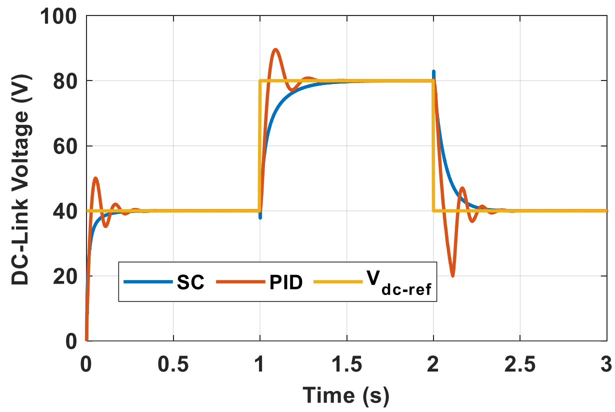

Fig. 4 – Output voltage of the DC-DC boost converter for reference voltage variations using the suggested SC algorithm and PID controller.

The next system test is the load resistor variation. In this test, the simulation time is 4s. After reaching the steady state, the load resistor value suddenly changes from 100 Ω to 50 Ω and inversely from 50 Ω to 100 Ω during the time [1.5, 3]s with a fixed output voltage at 40 V. Figure 5 shows that the output DC voltage remains constant at its reference with a small fluctuation during the load change.

Nevertheless, the suggested SC algorithm exhibits commendable robustness in such disturbances. Despite the overshoots/undershoots, the proposed SC algorithm selectively maintains stability and demonstrates resilience in handling these disturbances.

The proposed SC algorithm performs better than the PID controller in robustness and fast recovery time. At time t = 1.5 s, when the load resistance variation is raised, the output voltage deviation of the SC algorithm is smaller (5.32 V) than that of the PID controller (8.73 V).

In addition, the SC algorithm's recovery time is less (0.38 s) than that of the PID controller (0.68 s). Next, the load resistance variation is reduced at time t = 3 s; in this condition, the output voltage deviation of the SC algorithm is smaller, 6.08 V, than that of the PID controller, 11.33 V. Furthermore, the recovery time of the SC algorithm is smaller, 0.28 s, than that of the PID controller, 0.3 ms.

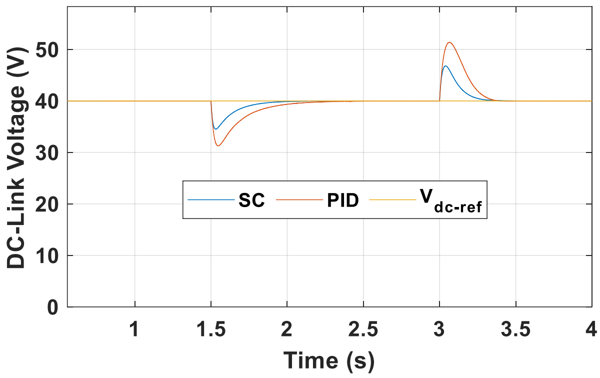

Fig. 5 – Output voltage of the DC-DC boost converter for load resistance variations using the suggested SC algorithm and PID controller.

To prove the proposed SC method's advantages, Table 2 compares the change of reference output voltage (ΔV_{dc}) and its recovery time (t_r) for both the steady and transient states.

The comparisons in Table 2 are based on two cases: the change of DC load and the change of reference output voltage. The comparison confirms the importance of the proposed SC method when the overshoot in output voltage is enhanced. Moreover, the response time is very acceptable.

Table 2

Transient values corresponding to test 2 and test 3 and its comparison

	Increasing load		Decreasing load		Overshoot	Undershoot
	ΔV_{dc} (V)	t_r(s)	ΔV_{dc}(V)	t_r(s)	ΔV_{dc}(V)	ΔV_{dc}(V)
SC method	5.32	0.38	6.08	0.28	-	-
Ref [27]	8.62	0.30	9.75	0.33	10	10
Ref [28]	4.20	0.08	6.57	0.31	-	4
Ref [29]	2.50	0.40	7.34	0.38	-	-

5. EXPERIMENTAL VERIFICATIONS

Figure 6 depicts an experimental setup designed to evaluate and verify the feasibility of the proposed control technique using dSPACE DS1104. Table 1 shows the main parameters of the experimental prototype.

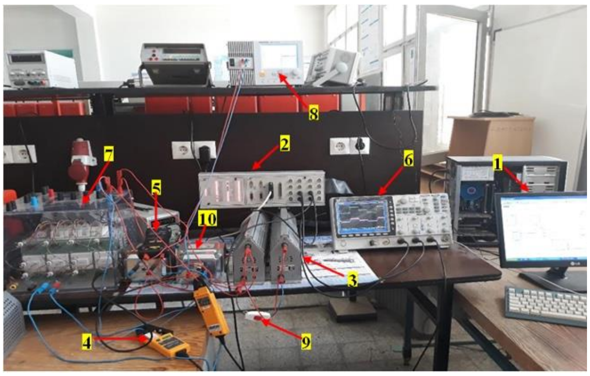

Fig. 6 – Hardware prototype built to evaluate the proposed method; 1 – PC; 2 – dSPACE; 3 – load; 4 – current sensor; 5 – Voltage sensor; 6 – oscilloscope; 7 – SEMISTACK-IGBT inverter; 8 – DC power supply; 9 – manual switch; 10 – inductor.

The controlled system's robustness was tested under abrupt output voltage and load disturbances. Figures 7–10 illustrate the experimental results and capabilities of the controller under abrupt variations in the output voltage and load.

5.1. PERFORMANCE UNDER DC VOLTAGE VARIATION

This test describes the possible circumstances at different reference output voltages, as portrayed in Figs. 7 and 8. Figure 7 considers a sudden rise and dip in the reference output voltage from 40 V to 80 V and inversely under full load conditions.

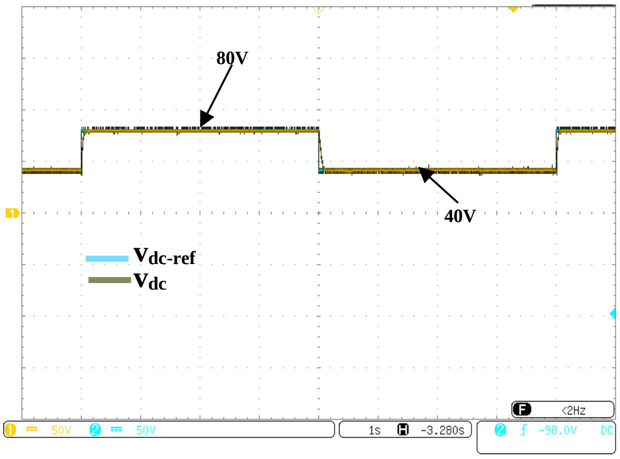

Fig. 7 – Experimental of the output voltage transient responses during a reference voltage change from 40 V to 80 V and vice versa.

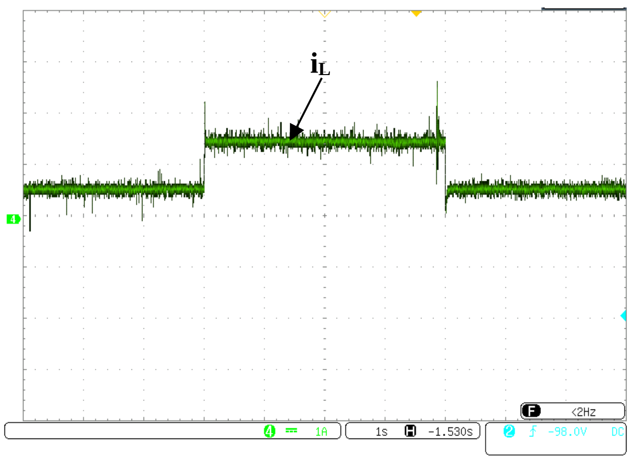

Fig. 8 – Experimental transient responses of inductor current during a reference voltage change.

The proposed technique diminishes the voltage overshoot and settling time considerably. The under/overshoot is 0.2 % / 0.1 %, respectively, with a settling time of 100 ms / 128 ms when increasing/ decreasing the output voltage.

It demonstrates the proposed control technique's suitable transient response. From this test, the SC can track the reference output voltage of the DC/DC boost converter with fast response time and low under/overshoot.

5.2. PERFORMANCE UNDER LOAD VARIATIONS

To further verify the robustness of the proposed SC controller against the load changes, it is examined. To investigate this issue, the experimental setup is evaluated by varying the load with a fixed output voltage at 40 V. Figures 9 and 10 show the responses of the output DC-link voltage and inductor current of the DC/DC boost converter after a step change of 50% in the load. SC can quickly restore the output voltage to the nominal value, and the overshoot is small. Based on this test, the proposed control scheme can meet the abrupt load demand.

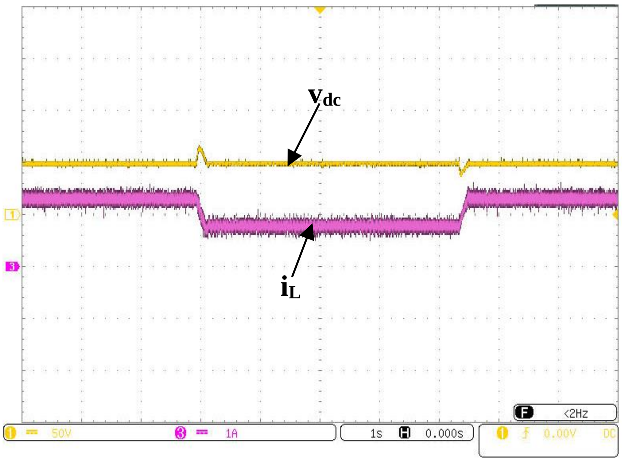

Fig. 9 – Transient response of the boost converter with a step change of 5[illegible] the load.

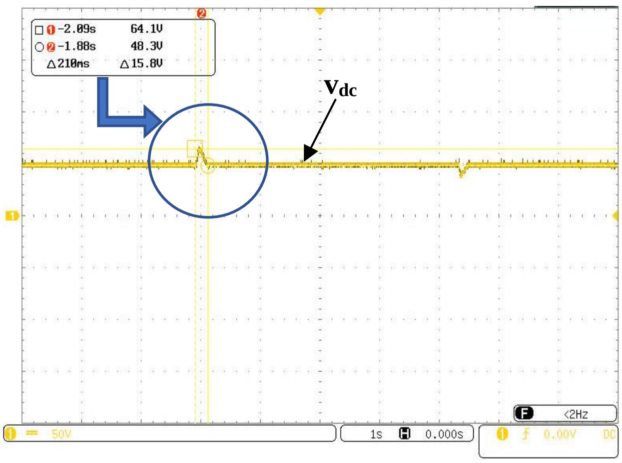

Fig. 10 – Response time and overshot values during load changes.

6. CONCLUSIONS

Inspired by SMC, a high-efficiency boost converter with the most cost-effective scheme based on SC theory was presented in this paper. The controlled system was subjected to set point tracking changes such as load and output voltage variations. The studied system was tested by simulations and experiments around the DSPACE 1104 control board. The simulation and experiment results showed acceptable performances of the proposed control method in the steady state and transients. Different performances of the control strategy, such as tracking ability, fast convergence, and law under/overshoot, were demonstrated in experimental and simulation tests. Finally, due to its robustness and performance, the suggested controller is worth recommending to other industrial applications with nonlinearities and disturbances.

Received on 1 August 2023

REFERENCES

1. H.W. Choi, S.M. Kim, J. Kim et al., *Current-balancing strategy for multileg interleaved DC/DC converters of electric-vehicle chargers*, Journal of Power Electronics, **21**, pp. 94–102 (2021).
2. P.S. Tomar, M. Srivastava, A.K. Verma, *An improved current-fed bidirectional DC–DC converter for reconfigurable split battery in EVs*, IEEE Transactions on Industry Applications, **56**, *6*, pp. 6957–6967 (2020).
3. N.V. Sang, W. Choi, D. Kim, *Non-isolated boost charger for the Li-ion batteries suitable for fuel cell powered laptop computers*, Journal of Power Electronics, **13**, *1*, pp. 31–3[illegible] (20[illegible]3).
4. K. Seba, M. Birane, K. Benmouiza, *A comparative analysis of boost converter topologies for photovoltaic systems using MPPT (PO) and beta methods under partial shading*, Rev. Roum. Sci. Techn. – Électrotechn. Et Énerg., **68**, *4*, pp. 375-380 (2023).
5. K. Yari, H. Mojallali, S.H. Shahalami, *A new coupled-inductor-based Buck–Boost DC–DC converter for PV applications*, IEEE Transactions on Power Electronics, **37**, *1*, pp. 687–69[illegible] (20[illegible]2).
6. M.I. Awaad, Z.E. Afifi, *Design, simulation and implementation of a DC microgrid based on quadruple DC converter*, Computers & Electrical Engineering, **89**, 106948 (2021).
7. S. H. Chincholkar, W. Jiang, C. Chan, *An improved PWM-based sliding-mode controller for a DC–DC cascade boost converter*, IEEE Transactions on Circuits and Systems II: Express Briefs, **65**, *11*, pp.1639–1643 (2018).
8. V. Repecho, D. Biel, J.M. Olm, E. Fossas, *Robust sliding mode control of a DC/DC Boost converter with switching frequency regulation*, Journal of the Franklin Institute, **355**, pp. 5367–538[illegible] (20[illegible]8).
9. J. Wang, W. Luo, J. Liu, L. Wu, *Adaptive type-2 FNN-based dynamic sliding mode control of DC–DC Boost converters*, IEEE Transactions on Systems, Man, and Cybernetics: Systems, **51**, *4*, pp. 2246–2257 (20[illegible]1).
10. S. H. Chincholkar, W. Jiang, C. Chan, *A modified hysteresis-modulation-based sliding mode control for improved performance in hybrid DC–DC Boost converter*, IEEE Transactions on Circuits and Systems II: Express Briefs, **65**, *11*, pp.1683–1687 (2018).
11. L. Cheng et al., *Model predictive control for DC–DC Boost converters with reduced-prediction horizon and constant switching frequency*, IEEE Transactions on Power Electronics, **33**, *10*, pp. 9064–9075 (2018).
12. O. Andrés-Martínez, A. Flores-Tlacuahuac, O.F. Ruiz-Martinez, J.C. Mayo-Maldonado, *Nonlinear model predictive stabilization of DC–DC Boost converters with constant power loads*, IEEE Journal of Emerging and Selected Topics in Power Electronics, **9**, *1*, pp. 822–830 (2021).
13. C.A. Torres-Pinzon, R. Giral, R. Leyva, *LMI-based robust controllers for dc-dc cascade boost converters*, Journal of Power Electronics, **12**, *4*, pp. 538–547 (2012).
14. Z. Salam, F. Taeed, S.M. Ayob, *Design and implementation of a single input fuzzy logic controller for boost converters*, Journal of Power Electronics, **11**, *4*, pp. 542–55[illegible] (20[illegible]1).
15. E. Santi, A. Monti, D. Li, K. Proddutur, R.A. Dougal, *Synergetic control for DC–DC Boost converter: implementation options*, IEEE Transactions on Industry Applications, **39**, *6*, pp. 1803–1813 (2003).
16. A. Kolesnikov, *Modern Applied Control Theory: Synergetic Approach in Control Theory*, TRTU, Moscow, Taganrog, 2000.
17. L. Xiao, L. Zhang, F. Gao, J. Qian, *Robust fault-tolerant synergetic control for dual three-phase PMSM drives considering speed sensor fault*, IEEE Access, **8**, pp. 78912–78922 (2020).
18. A.S. Malik, I. Ahmad, A. U. Rahman, Y. Islam, *Integral Backstepping and Synergetic Control of Magnetic Levitation System*, IEEE Access, **7**, pp. 173230–173239 (20[illegible]9).
19. N. Eghtedarpour, *A synergetic control architecture for the integration of photovoltaic generation and battery energy storage in DC microgrids*, Sustainable Energy, Grids and Networks, **20**, 100250 (2019).
20. C.H. Liu, M.Y. Hsiao, *A finite time synergetic control scheme for robot manipulators*, Computers & Mathematics with Applications, **64**, *5*, pp. 1163–1169 (2012).
21. R. Fazal, M.A. Choudhry, *Design of non-linear Static Var Compensator based on Synergetic Control Theory*, Electric Power Systems Research, **151**, pp. 243–250 (2017).
22. B. Babes, A. Boutaghane, N. Hamouda, M. Mezaache, S. Kahla, *A robust adaptive fuzzy fast terminal synergetic voltage control scheme for DC/DC buck converter*, International Conference on Advanced Electrical Engineering (ICAEE), 2019.
23. B. Babes, A. Boutaghane, N. Hamouda, *Design and real-time implementation of an adaptive fast terminal synergetic controller based on dual RBF neural networks for voltage control of DC–DC step-down converter*, Electrical Engineering, **104**, *2*, pp. 945–957. Springer Science and Business Media LLC, 2022.
24. B. Babes, N. Hamouda, F. Albalawi, O. Aissa, S.S.M. Ghoneim, S.A. M. Abdelwahab, *Experimental investigation of an adaptive fuzzy-neural fast terminal synergetic controller for buck DC/DC converters*, Sustainability, **14**, *13*, p. 7967. MDPI AG (2022).

25. N. Hamouda, B. Babes, *A DC/DC Buck Converter Voltage Regulation Using an Adaptive Fuzzy Fast Terminal Synergetic Control*, Lecture Notes in Electrical Engineering, Springer Nature Singapore, 2020, pp. 711–72[illegible]
26. S. Benaicha, *Robust sensorless speed control of an induction motor drive using a synergetic approach*, Rev. Roum. Sci. Techn. – Électrotechn. et Énerg., **68**,*4*, pp. 381-387 (2023).
27. S. Azarastemal, M. Hejri, *Cascade control system design and stability analysis for a DC–DC Boost converter with proportional integral and sliding mode controllers and using singular perturbation theory*, Iran J. Sci. Technol. Trans. Electr. Eng., **45**, pp.1445–1462 (2021).
28. A.Vazani, H.Mirshekali, N.Mijatovic, V.Ghaffari et al., *Composite nonlinear feedback control of a DC-DC boost converter under input voltage and load variation*, International Journal of Electrical Power & Energy Systems, **155**, Part B, 109562 (2024).
29. Z.B. Duranay, H. Guldemir, S. Tuncer, *Fuzzy sliding mode control of DC-DC boost converter*, Eng. Technol. Appl. Sci. Res., **8**, *3*, pp. 3054–3059 (2018).